Determining the Scattering Properties of Vertically-Structured Nepheloid Layers from the Fusion of Active and Passive Optical Sensors

Curtis D. Mobley
Sequoia Scientific, Inc.
2700 Richards Road, Suite 107
Bellevue, WA 98005
phone: 425-641-0944 x 109 fax: 425-643-0595 email: curtis.mobley@sequoiasci.com

Award Number: N0001404M0108
http://www.onr.navy.mil/sci_tech/32/322/ocean_optics_biology.asp

LONG-TERM GOAL

The overall goal of this work, now completed, was to combine hyperspectral imagery (HSI) with LIDAR bathymetry to improve retrievals of bottom classification and water-column inherent optical properties including, if possible, the retrieval of the vertical structure of water-column and benthic-boundary scattering layers from airborne platforms.

OBJECTIVES

There are critical differences between active and passive systems, including the errors in their estimates of bathymetry, bottom classification, and water column inherent optical properties (IOPs). Active LIDAR systems have greater depth penetration and smaller errors associated with bathymetry estimates. In addition, these systems can be operated without regard to solar illumination and have fewer atmospheric constraints. Passive systems yield spectral data with lower power requirements and allow for the retrieval of bottom characteristics above and beyond bathymetry. However, the existing HSI inversion techniques that solve for bottom classification and in situ IOPs require a simultaneous solution for bathymetry. Inhomogeneous waters can introduce uncertainties into the spectrum-matching and look-up-table (LUT) approach of Mobley et al., 2005 that increase the errors in the simultaneous estimates of bathymetry, bottom classification, and in-water IOPs. One of the greatest attributes of the passive systems, however, is that they have far greater spatial coverage for the same hour of flight time. This yields a critical difference in the deployment strategies of these systems in that at the same ground resolution (a few meters) the hyperspectral systems have 30-40 times the spatial coverage of LIDAR systems. A method that fuses these techniques could provide the ability to cover thousands of square kilometers a day, possibly providing estimates of the vertical structure of IOPs, as well as bathymetry and bottom classification, with concomitant error budgets. This research therefore focused on developing deployment schemes and data fusion techniques for coupled active and passive sensor systems so as to address the above issues.

APPROACH

The spectrum-matching and look-up-table (LUT) methodology of Mobley et al., 2005 is based on comparing a measured remote-sensing reflectance spectrum with a large database of spectra corresponding to known water, bottom, and external environmental conditions. The water and bottom

Report Documentation Page

Form Approved
OMB No. 0704-0188

1. REPORT DATE **30 SEP 2006**	2. REPORT TYPE	3. DATES COVERED **00-00-2006 to 00-00-2006**

4. TITLE AND SUBTITLE **Determining the Scattering Properties of Vertically-Structured Nepheloid Layers from the Fusion of Active and Passive Optical Sensors**	5a. CONTRACT NUMBER 5b. GRANT NUMBER 5c. PROGRAM ELEMENT NUMBER
6. AUTHOR(S)	5d. PROJECT NUMBER 5e. TASK NUMBER 5f. WORK UNIT NUMBER
7. PERFORMING ORGANIZATION NAME(S) AND ADDRESS(ES) **Sequoia Scientific, Inc,2700 Richards Road, Suite 107,Bellevue,WA,98005**	8. PERFORMING ORGANIZATION REPORT NUMBER
9. SPONSORING/MONITORING AGENCY NAME(S) AND ADDRESS(ES)	10. SPONSOR/MONITOR'S ACRONYM(S) 11. SPONSOR/MONITOR'S REPORT NUMBER(S)

12. DISTRIBUTION/AVAILABILITY STATEMENT
Approved for public release; distribution unlimited

13. SUPPLEMENTARY NOTES

14. ABSTRACT

15. SUBJECT TERMS

16. SECURITY CLASSIFICATION OF:			17. LIMITATION OF ABSTRACT	18. NUMBER OF PAGES	19a. NAME OF RESPONSIBLE PERSON
a. REPORT **unclassified**	b. ABSTRACT **unclassified**	c. THIS PAGE **unclassified**	**Same as Report (SAR)**	**9**	

conditions of the water body where the spectrum was measured are then taken to be the same as the conditions corresponding to the database spectrum that most closely matches the measured spectrum.

To improve LUT retrievals of bottom and water-column optical properties, I developed code to constrain these retrievals by using known bathymetry as obtained from a LIDAR survey of the imaged area. I also investigated the retrieval of in-water and benthic boundary scattering layers using HSI.

The data set of combined LIDAR bathymetry and hyperspectral imagery (HSI), which was anticipated to be acquired by others in separately funded work, never became available. I therefore substituted an image from Lee Stocking Island, Bahamas, which was taken during the ONR-funded Coastal Benthic Optical Properties (CoBOP) program, for which acoustic bathymetry was available. Whether the bathymetry is available from LIDAR, an acoustic survey, or a digitized nautical chart is largely irrelevant when doing depth-constrained retrievals of bottom and water-column properties.

WORK COMPLETED

In related work this year on the LUT methodology (see separate annual report), I developed LUT R_{rs} inversion code that allows the depth to be either unknown or known at each pixel. When the depth is known for a given pixel, only the bottom reflectance and water-column absorption, scatter, and backscatter spectra are retrieved by the LUT inversion. If no depth is available for a given pixel, then the bathymetry is also retrieved. I then used that code in the present work investigate what improvements in LUT retrievals of bottom classification and water inherent optical properties (IOPs) can be achieved if the bathymetry is known from a LIDAR.

RESULTS

Figure 1 shows an RGB image of the Horseshoe Reef area north of Lee Stocking Island, Bahamas. Figure 2 shows the acoustic bathymetry coverage, which was used as a proxy for LIDAR bathymetry. The available acoustic coverage was interpolated from the acoustic ping locations to the HSI pixels, so that each pixel then had a known depth. Areas without acoustic coverage were masked out (the grey areas in the subsequent figures) and omitted from the subsequent analyses. The LUT retrieval then took the depth as known at each pixel, so that only the bottom reflectance and water-column absorption and scattering spectra needed to be retrieved by the LUT spectrum-matching algorithms.

Various LUT retrievals of bottom reflectance/type and water-column IOPs were made for unconstrained depths (i.e., LUT simultaneously retrieves the bottom depth along with the bottom reflectance and water-column IOPs) vs. constrained depths (the depth at each pixel is given by the interpolated acoustic bathymetry, so that LUT solves only for the bottom reflectance and water properties). Figures 3 and 4 show an example of the difference in the retrieved bottom reflectance R_b at 488 nm. Figure 5 shows the corresponding percent changes in $R_b(488)$. Constraining the depth caused some areas of highly reflecting bottom to get brighter, and some low-reflecting areas got darker, but on average the bottom reflectance changed by only +3%. Forty percent of the pixels had $R_b(488)$ change by less than ±5%, and only 11% of pixels changed by more that ±25%.

Figures 6 and 7 show the corresponding changes in bottom classification for unconstrained vs. constrained depths. We see that when the depth is constrained, some areas retrieved as dense vegetation are reclassified as pure corals or less dense mixtures of mixtures of sediment, corals, sea grass, turf algae, and macrophytes. Some areas originally classified as sand with sparse vegetation are reclassified as bare sediment when the depth is constrained. Overall, though, there are no large changes in the bottom classification.

Thus we see that constraining the depth causes some changes in the bottom retrieval, in terms of either the reflectance or the bottom type. This is what is expected. The constrained retrievals are likely more accurate, but pixel-by-pixel bottom reflectances or classification are not available for validation of these retrievals. In either case, the retrieved bottom classification is plausible.

However, the changes are not great. For example, a sediment bottom is never turned into dense vegetation or vice versa. The reason that the depth-constrained retrievals are not greatly different from the unconstrained retrievals is that the unconstrained LUT depth retrievals are already close to correct. (On average, the unconstrained LUT depth retrievals for this image were within 7% of the acoustic values, and 87% of the LUT retrievals were within 25% of the acoustic depth.) Constraining the depths to be exactly correct thus has only a small effect on the remaining parameters being retrieved. *This indicates that the LUT retrieval is not having any problems with non-uniqueness.* That is to say, LUT never finds an incorrect depth, incorrect bottom reflectance, and incorrect water IOPs that together give a remote-sensing reflectance that is close to the correct one. This is a reassuring check on LUT's ability to retrieve the correct environmental parameters in unconstrained retrievals, as will often be necessary in applications to denied-access areas.

Similar small changes are seen in the retrieved absorption, scattering, and backscatter spectra. These IOP retrievals are not shown here because of file size limitations for electronic submission of reports.

I thus conclude that constraining the depth can lead to improvements in the retrieved bottom classification and water IOPs, but that even unconstrained retrievals are acceptably accurate. In no instance does the LUT retrieval methodology have problems with the non-uniqueness of the remote-sensing reflectance spectra.

The results shown here will be presented in more detail at the Ocean Optics XVIII conference in October 2006. A paper on this work is being prepared for submission to either *Applied Optics* or *Optics Express*.

IMPACT/APPLICATION

This research leads to the ability to detect near-bottom scattering layers through the fusion of active and passive optical remote sensing data streams. This will provide needed IOP data, perhaps including IOP vertical structure when LIDAR data are available, for the performance prediction of both acoustic and optical MCM detection and identification systems. At the very least, these data streams will provide the information streams of bathymetry and bottom type, e.g. sand, mud, rock and clutter, necessary to support current Mine Warfare (MIW) decision aids. The use of hyperspectral sensors deployed on organic UAV platforms, coupled with airborne (e.g. LIDAR) or in-water estimates of bathymetry would allow for these information streams to be generated in near-real time in the littoral areas.

TRANSITIONS

The code and databases developed in this work were immediately passed on to P. Bissett and colleagues at the Florida Environmental Research Institute, who were responsible for the LIDAR aspects of this work and who collaborate on the further development of the LUT methodology for processing HSI.

RELATED PROJECTS

This work dovetailed with the further development of the LUT methodology, which is separately funded. My work was conducted in conjunction with Drs. Paul Bissett and Dave Kohler of the Florida Environmental Research Institute, who were separately funded for this collaboration. FERI was developing techniques for the fusion of LIDAR and hyperspectral imagery, focusing on the time-gated LIDAR signals combined with the application of the inversion techniques (LUT, optimization, and genetic algorithms) using known bathymetry.

REFERENCE

Mobley, C. D., L. K. Sundman, C. O. Davis, T. V. Downes, R. A. Leathers, M. J. Montes, J. H. Bowles, W. P. Bissett, D. D. R. Kohler, R. P. Reid, E. M. Louchard, and A. Gleason, 2005. Interpretation of hyperspectral remote-sensing imagery via spectrum matching and look-up tables. *Applied Optics* **44**(17), 3576-3592.

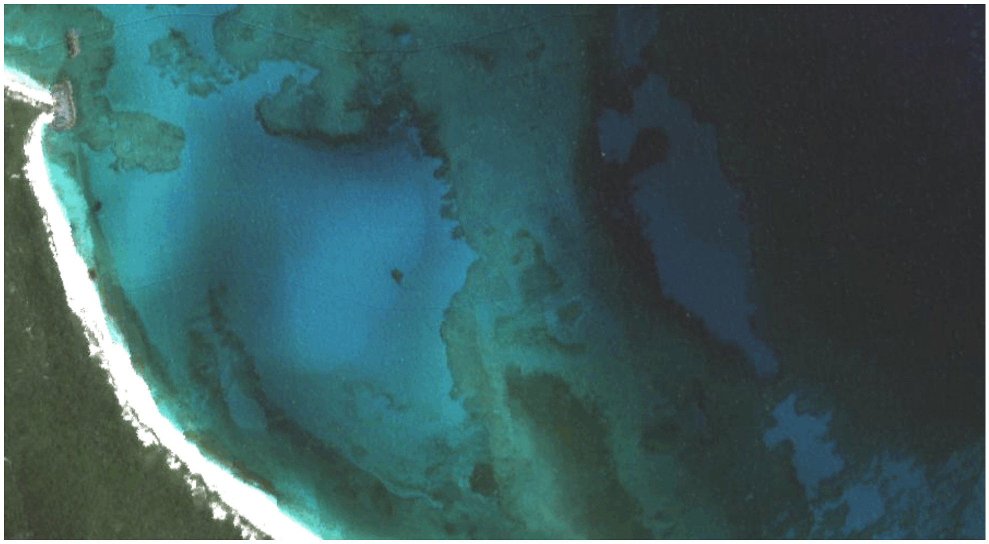

Fig. 1. An RGB image of the Horseshoe Reef area made from a PHILLS hyperspectral image taken May 20, 2000. The bottom includes areas of highly reflecting ooid sands, low reflecting, dense sea grass beds, and intermediate reflecting areas of mixed sediments, corals, sea grass, turf algae, and macrophytes.

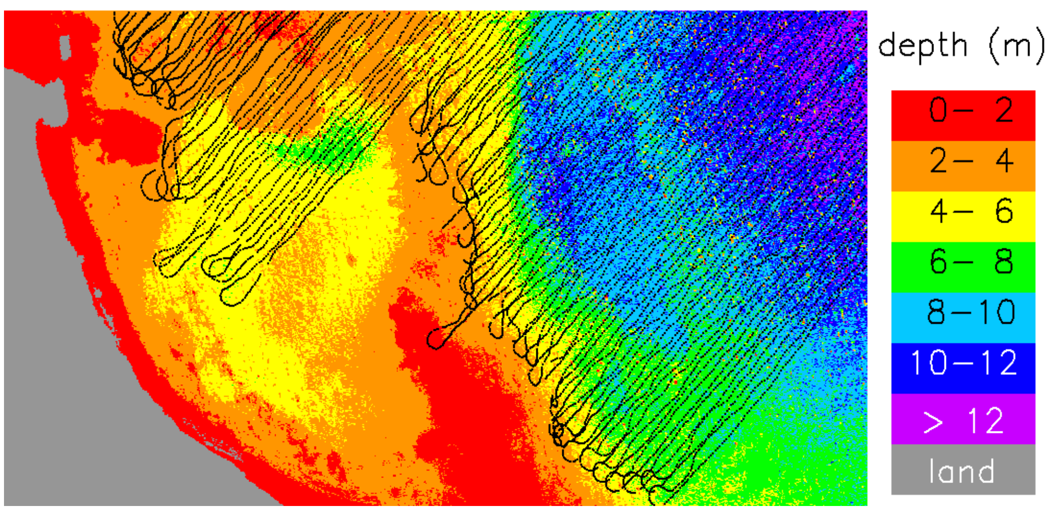

Fig. 2. Acoustic bathymetry coverage for the area corresponding to Fig. 1. The black dots show the locations of the acoustic pings. The depth at each pixel of the image of Fig. 1 is obtained by interpolation between the locations of the acoustic data, where available. Regions for which no acoustic data are available are omitted from further analysis. The color-coded depths are for the unconstrained LUT retrieval applied to the entire image.

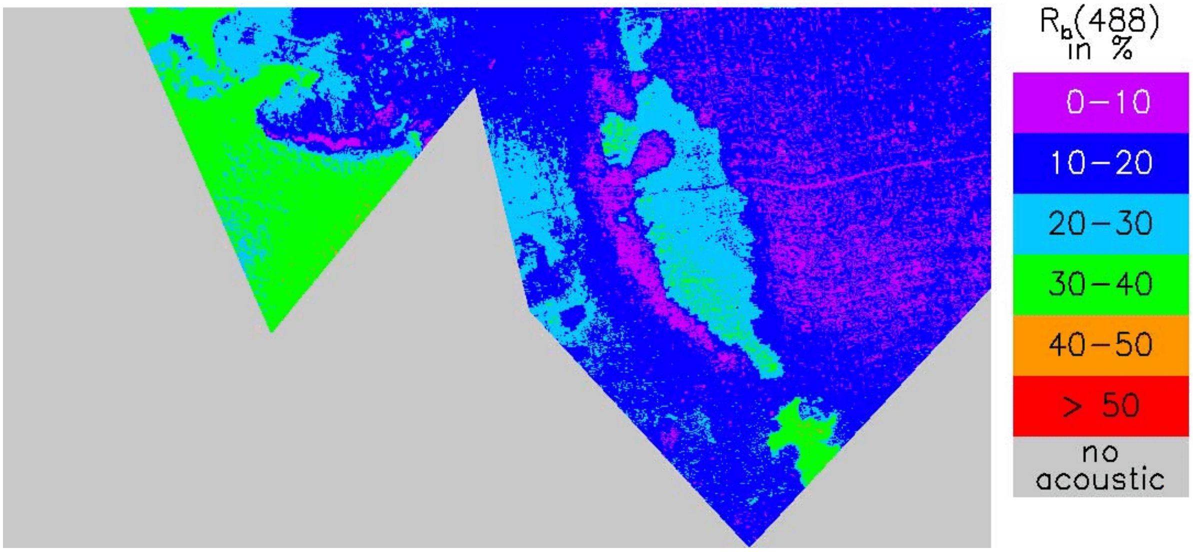

Fig. 3. Bottom reflectance R_b at 488 nm obtained by LUT in an unconstrained retrieval. The gray area does not have acoustic coverage.

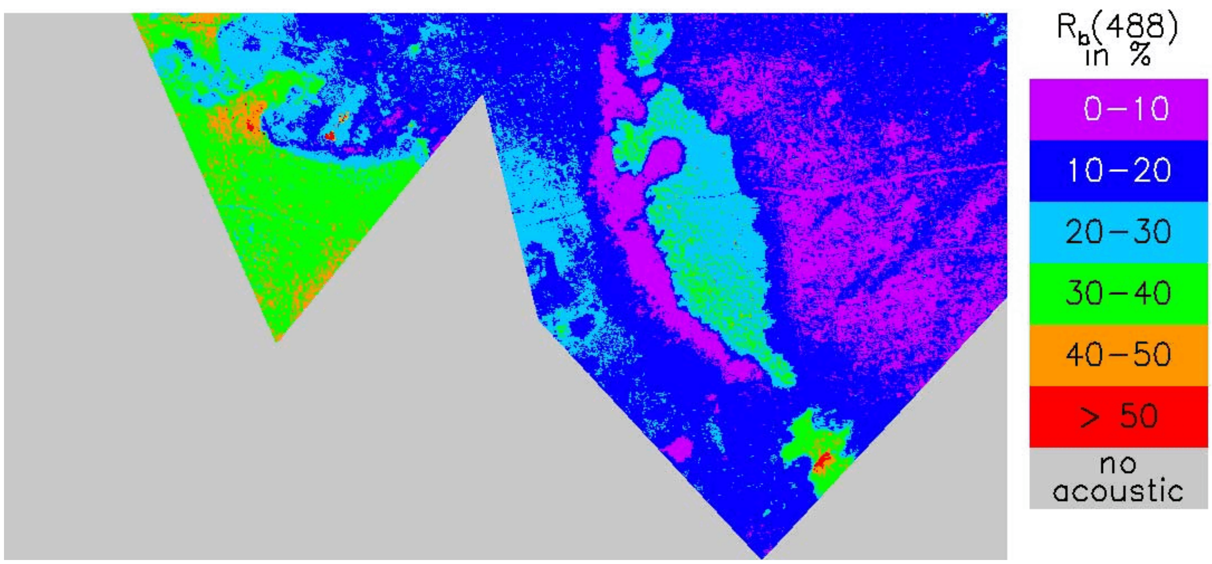

Fig. 4. Bottom reflectance R_b at 488 nm obtained by LUT in a depth-constrained retrieval, i.e., when the bottom depth at each pixel is given by the acoustic bathymetry.

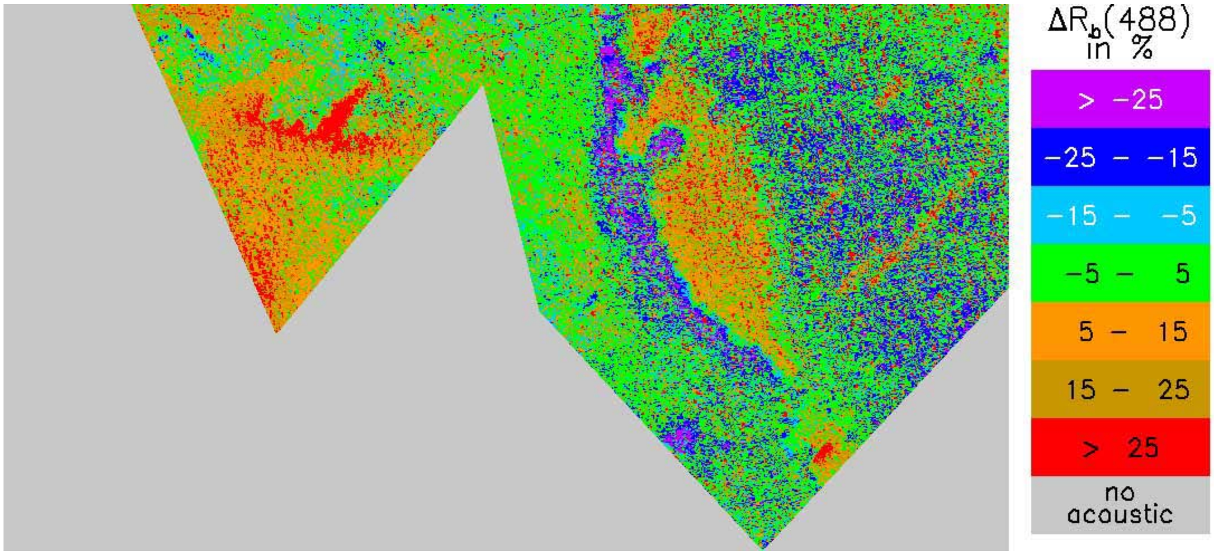

Fig. 5. Percent change in bottom reflectance R_b at 488 nm for the depth-constrained vs. unconstrained retrievals of Figs. 3 and 4. Negative changes mean the bottom got darker (less reflective); positive changes mean the bottom got brighter (more reflective).

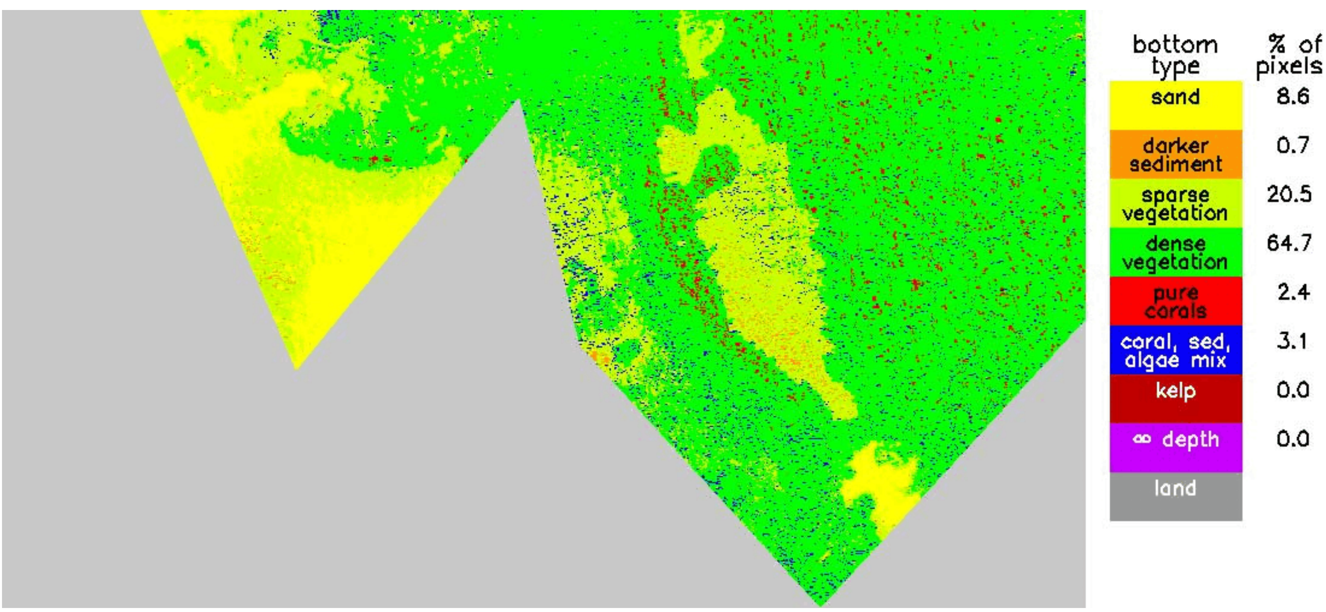

Fig. 6. Bottom classification for the unconstrained retrieval.

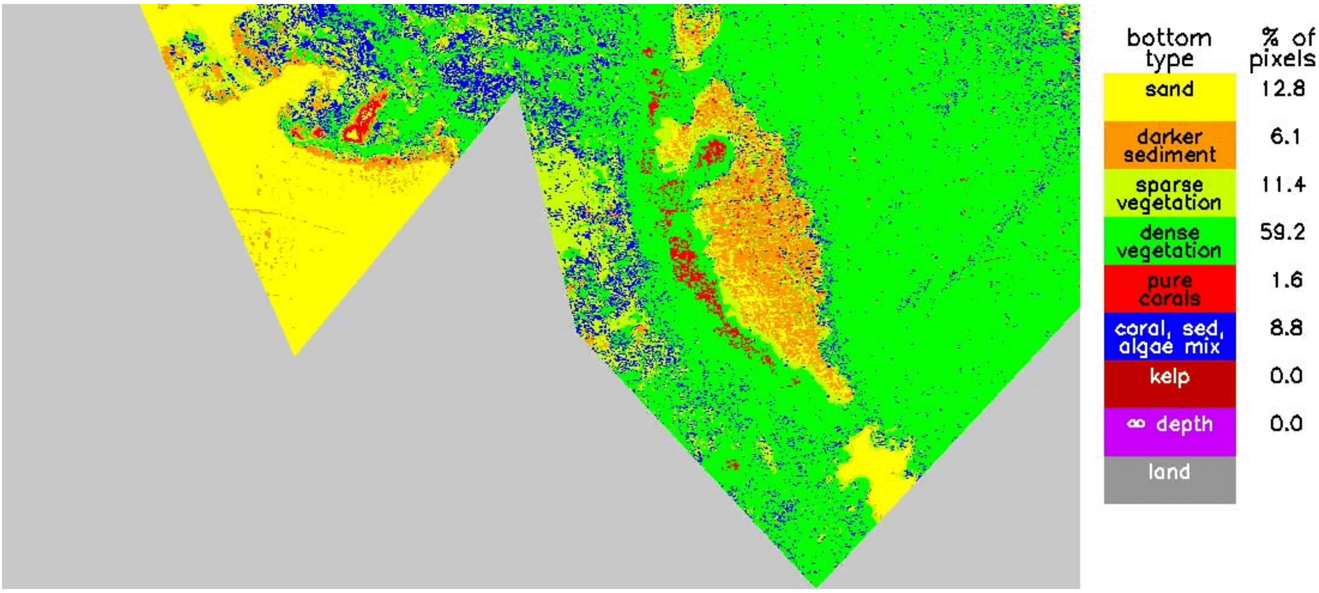

Fig. 7. Bottom classification for the depth-constrained retrieval.